УДК 624.07 DOI: 10.33979/2073-7416-2023-110-6-58-72

H.H. ALZAMILI[1], A.M. ELSHEIKH[1,2]
[1]Peoples' Friendship University of Russia (RUDN University), Moscow, Russia
[2]Mansoura University, Mansoura, Egypt

NUMERICAL STUDY OF THE BEHAVIOR OF RC BEAM AT HIGH TEMPERATURES

Abstract. *The numerical study focuses on analyzing the structural response of reinforced concrete (RC) beams at high temperatures. Gaining more insight into the behavior of reinforced concrete (RC) structures at high temperatures and the material properties of steel reinforcement and concrete are the main goals of this research. To conduct this analysis, finite element analysis (FEA) using the ABAQUS software package is adopted. FEA allows for the simulation of the behavior of the RC beam under fire by inputting relevant parameters, such as material properties, dimensions, and temperature. The program calculates the temperature distribution within the structure and predicts the resulting structural responses. Two phases are applied: before and after exposure to fire. Both normal-strength concrete (NSC) beams and high-strength concrete (HSC) beams are considered. The results indicate that high temperatures have a detrimental effect on the overall behavior of concrete beams. At 600°C, the residual strength of HSC beams is shown to be twice that of NSC beams.*

Keywords: *beam, concrete, fire, strength, ABAQUS.*

Х.Х. АЛЬЗАМИЛИ[1], А.М. ЭЛЬШЕЙХ[1,2]
[1]Российский университет дружбы народов (РУДН), Москва, Россия
[2]Мансура университет, Мансура, Египет

ЧИСЛЕННОЕ ИССЛЕДОВАНИЕ ПОВЕДЕНИЯ ЖЕЛЕЗОБЕТОННЫХ БАЛОК ПРИ ВЫСОКИХ ТЕМПЕРАТУРАХ

Аннотация. *Численное исследование сосредоточено на анализе структурной реакции железобетонных (RC) балок при высоких температурах. Целью этого исследования является более глубокое понимание того, как железобетонные конструкции ведут себя при воздействии повышенных температур и как это влияет на свойства материалов бетона и стальной арматуры. Для проведения этого анализа используется анализ методом конечных элементов (FEA) с использованием пакета программного обеспечения ABAQUS. FEA позволяет моделировать поведение RC-балки под пожаром путем ввода соответствующих параметров, таких как свойства материала, размеры и температура. Программа рассчитывает распределение температуры внутри конструкции и прогнозирует результирующие структурные реакции. Применяются две фазы: до и после воздействия пожара. Рассматриваются балки как из нормального бетона (NSC), так и из высокопрочного бетона (HSC). Результаты показывают, что высокие температуры оказывают пагубное влияние на общее поведение бетонных балок. Показано, что при 600°C остаточная прочность балок HSC в два раза выше, чем балок NSC.*

Ключевые слова: *балка, железобетон, пожар, прочность, ABAQUS.*

Introduction

When concrete is exposed to high temperatures, it undergoes physical and chemical changes that can have a negative effect on its structural integrity [1]. The severity of these effects depends on the level and duration of the elevated temperatures. The main changes that occur are a loss of strength. Concrete loses its compressive and tensile strength at high temperatures.

This is primarily due to the dehydration of the cement paste, which leads to a decrease in the bond strength between the aggregates and the paste [2, 3].

As well as the most important changes that occur in concrete, it expands when exposed to high temperatures due to the thermal expansion of the constituent materials. This thermal expansion can lead to internal stresses and strains, resulting in cracking and spalling of the concrete [4].

Understanding how material properties change at elevated temperatures is crucial for assessing the behavior of fire-damaged constructions. When concrete is exposed to high temperatures. Thus, methods for the post-fire restoration of structural members are becoming more and more necessary in order to improve the structural safety of such members. Since several years ago, there has been a noticeable increase in the number of fire incidents in Iraq, which typically affect public markets, businesses, and government buildings. Each year, there are considerable losses in both lives lost and property lost as a result of these fire occurrences.

Concrete tunnel linings face significant challenges when exposed to fire. The behavior of these linings depends on factors such as fire duration, intensity, and concrete composition. Understanding the material properties and utilizing finite element simulations are crucial for evaluating the fire resistance and structural integrity of concrete tunnel linings. Advancements in simulation techniques contribute to better fire safety design and aid in formulating efficient fire protection strategies for tunnels [5].

Gao et al. [6] conducted a study on fire-exposed reinforced concrete beams using finite element modeling to assess the fire resistance of these beams and evaluate their structural response under different fire scenarios. The finite element model incorporates the geometric properties of the beams, the material properties of concrete and reinforcement, and the appropriate fire temperature-time curve.

Bin Cai et al. [7] conducted calculations and utilized a finite element analysis (FEA) method to assess the residual flexural capacity of post-fire RC beams. They also considered various factors for parametric studies on fire using the proposed FE model. Through their research, they found that the thickness of the concrete cover, longitudinal steel reinforcement ratio, fire exposure time, and fire exposure sides are the key parameters influencing the fire resistance of the beams. Figure 1 displays the temperature over time curve used in their study.

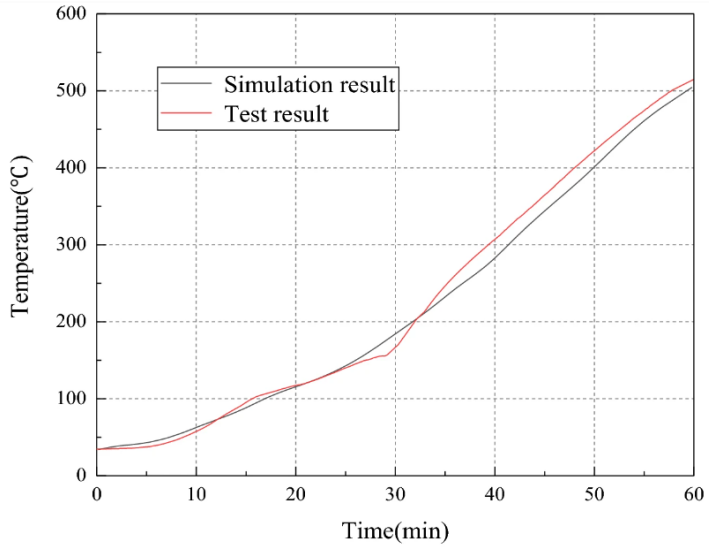

Figure 1 - Temperature–time curve [7]

Sajjad and Taher [8] focused on evaluating the impact of fire on reinforced concrete columns using the finite element method. They used the ABAQUS software for finite element analysis and validated their findings with experimental data. The columns were subject to a maximum temperature of 600 degrees Celsius for varying durations of 10, 15, and 20 minutes. Figure 2 illustrates the comparison of stiffness between the experimental and finite element results obtained from their study.

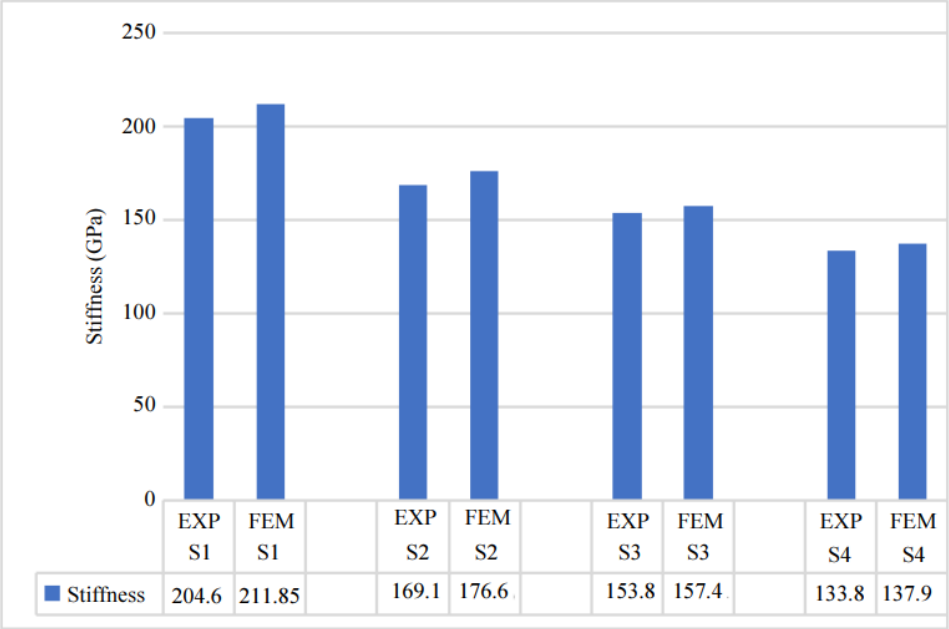

Figure 2 - Stiffness at different fire periods [27]

They found a strong correlation between the finite element (FE) analysis and experimental values in their study. The results demonstrated that the stiffness of reinforced concrete columns decreased as the duration of fire stress increased.

The methods used to model and analyze the behavior of the examined concrete element under various loading methods are presented and illustrated in this work. Numerical solver software development has been made easier by the widespread availability of computer devices and their recent advancements. ABAQUS is among the most powerful software programs that Simulia has created recently.

ABAQUS offers a range of tools and features to analyze various structural and thermal problems. It allows for the creation of detailed finite element models, the definition of material properties, and the application of thermal and mechanical loads. Additionally, the software provides post-processing capabilities to analyze and interpret the results obtained from the simulations [9].

In addition to having the capability to import components from other programs, like AutoCAD, with appropriate and different file extensions, ABAQUS also offers a flexible platform for modeling. Typically, the process for geometrical modeling involved creating individual parts based on their types, such as 3D, 2D, or 1D part. Moreover, some of parts are deformable, some others are rigid parts according to the simulation status [10].

The authors' approach of modeling steel bars as wire elements (1D parts) in the ABAQUS software package is a common simplification technique used to reduce computational time and complexity in structural analysis.

In many cases, especially when the focus is on the overall behavior of the reinforced concrete structure and not specifically on the steel-concrete interaction, modeling the steel bars as 1D elements is sufficient and efficient. By representing the steel bars as wire elements, the computational effort required to simulate the behavior of the individual steel bars is reduced compared to modeling them as full 3D elements [30].

This simplification is often justified when the mechanical properties of the steel bars, such as their Young's modulus and yield strength, are the main factors influencing the structural response.

The wire element approach allows for capturing the axial deformation and buckling behavior of the steel bars, which are the primary modes of deformation in most cases [11, 12].

Methods and Materials

Finite Element Modeling with ABAQUS

This study will provide a detailed description and discussion of the stages of modeling and simulation for the samples. The procedure is divided into two primary steps: simulation for the concrete beam samples that are exposed to high temperatures, and modeling and simulation for the reference samples, which are not fired concrete elements. To recreate any process or behavior of concrete elements using ABAQUS, the following key steps must be taken: part modeling; material properties; assembly; step; constraints and interaction properties; loading and boundary conditions; predefined field; and job [12].

Materials models and assigned section

The CDP (Concrete Damage Plasticity) model is a widely used constitutive model to simulate the behavior of concrete under various loading conditions. When using the CDP model for unfired concrete, it must define specific material parameters to accurately capture its behavior. Such as Young's modulus and Poisson's ratio. These parameters represent the stiffness and deformation characteristics of the material. In the plastic range, the stress-strain curve represents the nonlinear behavior of concrete as it undergoes deformation and damage. The CDP model takes into account the plastic behavior of concrete, which is characterized by parameters such as the compressive strength, tensile strength, fracture energy, and damage parameters.

By combining the elastic and plastic behavior, the CDP model can accurately simulate the response of concrete under different loading conditions, such as compressive loading. [13].

It's important to note that material parameters for unfired concrete may vary depending on factors such as the composition of the concrete mix, curing conditions, and specific test data. Experimental testing or established guidelines can help determine the appropriate values for these parameters [14]. The Selected CDP material parameters for unfired concrete are shown in table 1.

Table 1 - Selected CDP material parameter for unfired concrete

Parameter	Selected value
Material model	CDP model
E, MPa	23500 MPa for C25 and 38000 MPa for C65
Possion’s ratio	varying based on the temperature
Dilation angel	30 for C25 MPa and 40 for C65
*Ecc	0.1
*Fb0/fc0	1.16
*K	2/3
*Viscosity parameter	0.001

*As recommended by Abaqus manual

It is necessary to enter a more substantial curve into the CDP model (20 °C) that represents the uniaxial, unconfined stress-strain behavior under compressive conditions at ambient temperature. Figure 3 shows an illustration of the unconfined compressive stress-strain of both normal and high-strength concrete. By utilizing the CDP model, these curves can be classified as plastic or elastic, depending on the elasticity modulus and Possion's ratio.

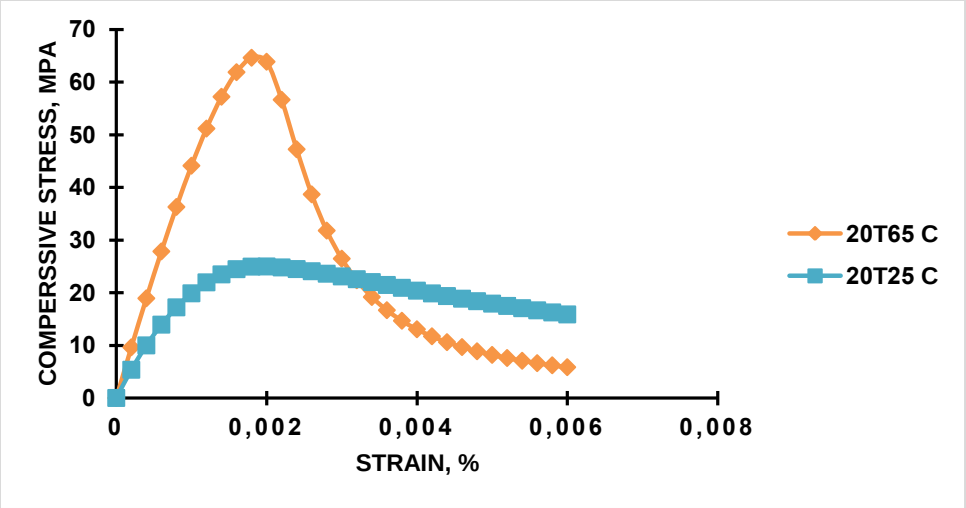

Figure 3 - Uniaxial concrete compressive stress- strain at ambient temperature (20C) for normal (25 MPa) and high (65 MPa) strength concrete class

Defining Steel material behavior

This study has exploited the elastic-perfectly plastic behavior of steel reinforcing rebar. This behavior assumes that the steel rebar behaves elastically up to its yield point and then exhibits perfect plasticity, meaning it undergoes permanent deformation without any further increase in stress.

To accurately define the elastic and plastic behavior of the steel rebar in the CDP model, it is necessary to have at least one point at the yielding stage, which corresponds to zero plastic strain. This point is crucial, as it helps determine the yield strength of the rebar [15].

Additionally, for the plastic phase, linear hardening points are required as a minimum. These points include the yield point and the rupture point. The yield point provides information about the onset of plastic deformation, while the rupture point represents the ultimate strength of the rebar before failure (see figure 4).

On the other hand, as shown in (table 2) points are required for the linear hardening of the plastic phase as a minimum: the yield point and the rapture point (2).

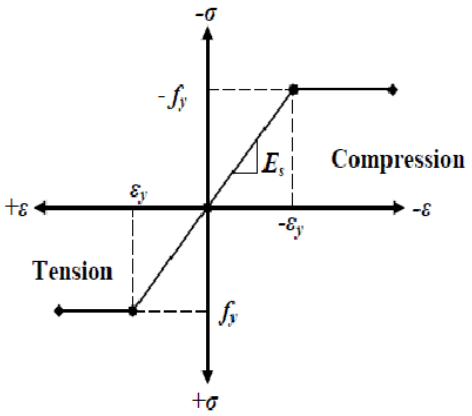

Figure 4 - Elastic perfect plastic behavior of steel reinforcement [16]

Table 2 - Parameters for define elastic perfect plastic model

Parameter	Selected value
Model type	Elastic perfect plastic behavior
E, MPa	200000
Yield stress, MPa	480
Possons ratio	0.3

Analysis and Results

Concrete element dimensions and cross sections

To demonstrate the effect of fire impact that occurred frequently in some infrastructure facilities such as hospitals, the beam has a full-scale dimension of 5500 mm in length, 300 mm in width, and 500 mm in thickness. The beam is reinforced with three steel bars at the top and bottom, each having a diameter of 16 mm. Additionally, transverse reinforcement in the form of stirrups is used along the length of the beam. The stirrups have a constant spacing of 200 mm and are made of steel bars with a diameter of 10 mm (see figure 5).

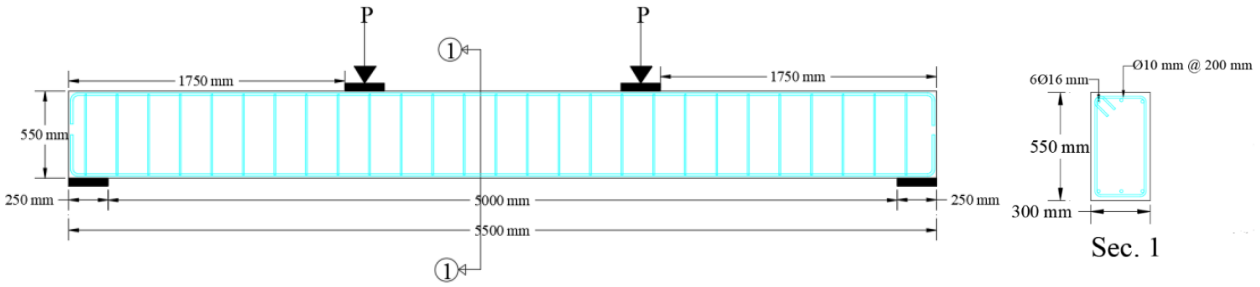

Figure 5 - The adopted full-scale dimensions and reinforcement of beam

Modeling of reference concrete beam samples (first phase)

Three components are needed to produce a geometrical model of the beam: loading and supporting plates, steel reinforcement, and the concrete beam. It is required that the simulation procedure for every generated part be carried out in three dimensions.

In particular, the concrete beam is made using the extraction process to build 3D deformable parts. This entails determining the proper extraction length for each component and drawing the beam's cross-section in the XY plane. 3D items having a straight longitudinal profile are frequently worked on using this technique.

A 1D wire method is applied to the steel reinforcement. This indicates that one-dimensional elements are used in the modeling of the steel reinforcement, including longitudinal bars and ties. This method makes the modeling process easier for for the intricate arrangement of reinforcement (see figure 6) [29].

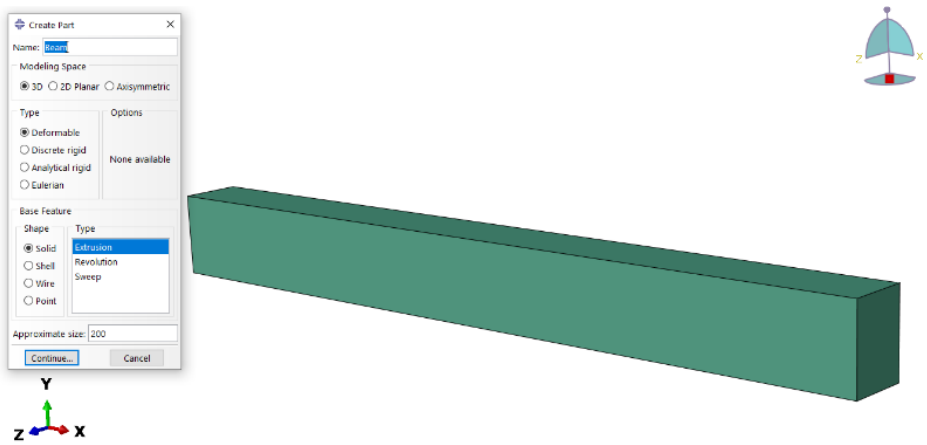

Figure 6 - Beam modelling in ABAQUS

Using the instances assembly module, the assembled parts were put into the simulation environment. After inserting the concrete beam, the long steel bars for the top and bottom layers together with the stirrups are positioned and duplicated, in accordance with the relevant simulation, which shows that this module builds, translates, rotates, or duplicates instances (see figure 7). It is noteworthy that, as a case study, ABAQUS provides an extruded view for wire elements exclusively.

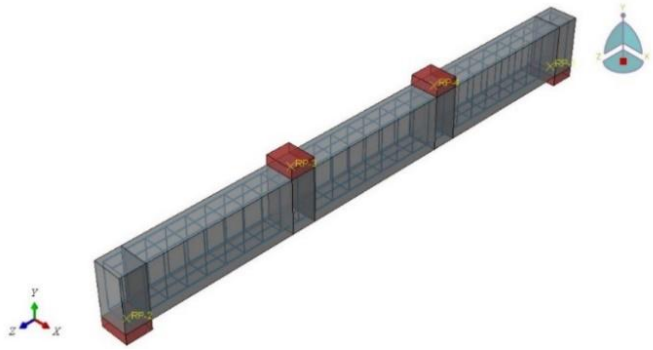

Figure 7 - Part assembling of beam

ABAQUS was used to conduct a heat transfer study to acquire the temperature fields of RC beams. The basis of the analysis is the determination of the thermal conductivity, materials' specific heat capacity, and density (see figures 8, 9, and 10) [17]. The parameters in equation (1) were chosen in accordance with Wang and He (2009). The thermal conductivity of concrete λcT (W/(m °C)) is where T is the temperature, °C.

$$\lambda_{cT} = 2 - 0.24(\frac{T}{120}) + 0.012(\frac{T}{120})^2 (20°C \leq T \leq 1200°C) \quad (1)$$

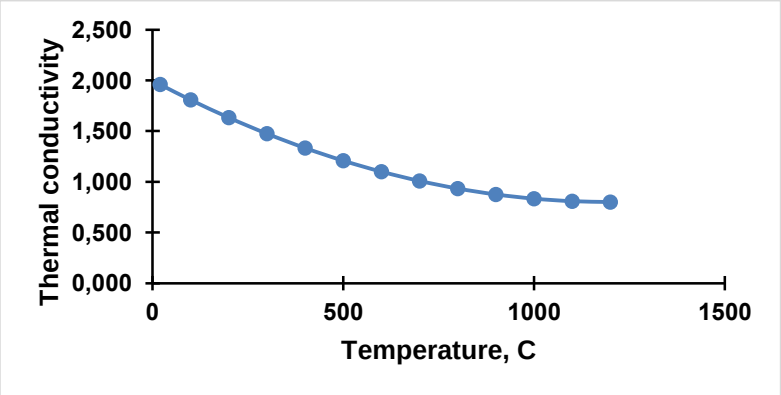

Figure 8 - Concrete thermal conductivity vs. temperature

The specific heat capacity of concrete CcT (J/(Kg °C)) is as shown in equation (2).

$$C_{cT} = 900 + 80\left(\frac{T}{120}\right) - 4\left(\frac{T}{120}\right)^2 \quad (20°C \leq T \leq 1200°C) \quad (2)$$

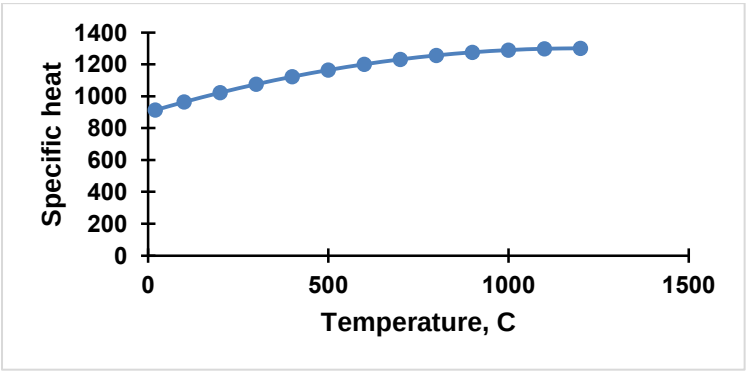

Figure 9 - Concrete specific heat vs. temperature

The density of concrete also changes as the temperature rises, so the equations (3), (4), (5) and (6) are used to define this characteristic in Kg/m^3 at higher temperatures [18]:

$$\rho_\theta = \rho_{20°C} = 2300 \text{ kg/m}^3 \quad 20°C \le \theta \le 115°C \tag{3}$$

$$\rho_\theta = \rho_{20°C} \cdot [1 - 0.02(\theta - 115)/85] \quad 115°C \le \theta \le 200°C \tag{4}$$

$$\rho_\theta = \rho_{20°C} \cdot \left[0.98 - \frac{0.03(\theta - 200)}{200}\right] \quad 200°C \le \theta \le 400°C \tag{5}$$

$$\rho_\theta = \rho_{20°C} \cdot [0.95 - 0.07(\theta - 400)/800] \quad 400°C \le \theta \le 1200°C \tag{6}$$

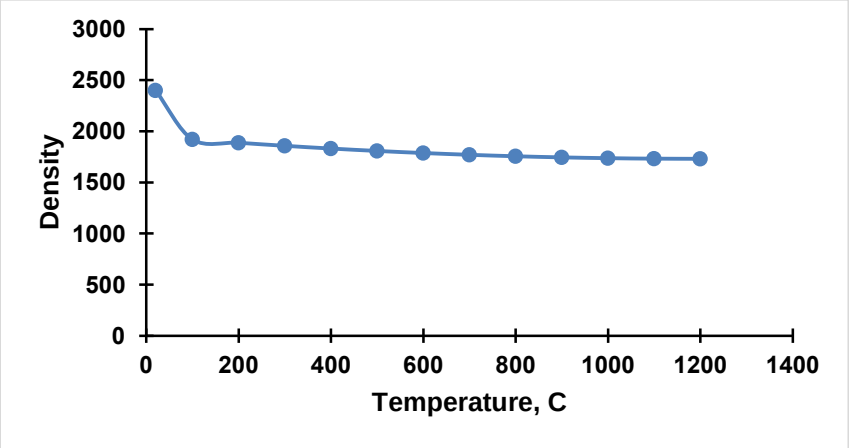

Figure 10 - Concrete density variations with high temperatures

The (step) analysis used the thermal analysis approach to simulate the distribution of heat on the fired beam. The transitory approach has been chosen for solving the problem. The goal of this type of analysis is to display the temperature distribution on the beam, and it took 7200 seconds, or two hours, in total.

To simulate heat convection between the ambient air temperature and a concrete beam. In order to simulate this heat transfer process, surface film conditions were assigned to the concrete sides and bottom edges of the beam.

To simulate the initial air temperature, a sink temperature of 20°C was set. This represents the temperature of the surrounding air before any heating or firing occurs. The heat amplitude of TC1 was used to represent the increase in temperature due to firing, indicating the rise in surrounding temperature.

For thermal analysis, conductivity was used to simulate how heat is transferred between different objects, such as steel and concrete. The conductivity value represents the ability of a material to conduct heat [19].

Furthermore, the surface film condition was used to simulate the interaction between the model and the surrounding media. The values recommended for surface film conditions depend on the surface being subject to fire or being unfired. As per the recommendations provided by the Fib modal code, a surface film condition value of 25 W/m^2 is suggested for surfaces subject to fire, while a value of 9 W/m^2 is recommended for unfired surfaces, as per ASTM E119.

Additionally, the temperature evolution of the Cellulosic Fire Curve (ISO-834) is described by the equation (7). The ISO curve describes the typical temperature profile observed during a cellulosic fire [20].

$$T = T_0 + 345\lg(8t + 1) \quad (7)$$

It is shown in (figure 11) that the temperature reached 745°C after 30 minutes, and that it rises by around 100°C each time the duration is doubled. The equation shows two stages of a fire: the flashover, which is characterized by a rapid temperature rise to about 800°C, and the subsequent phase, which is characterized by the fire's full formation.

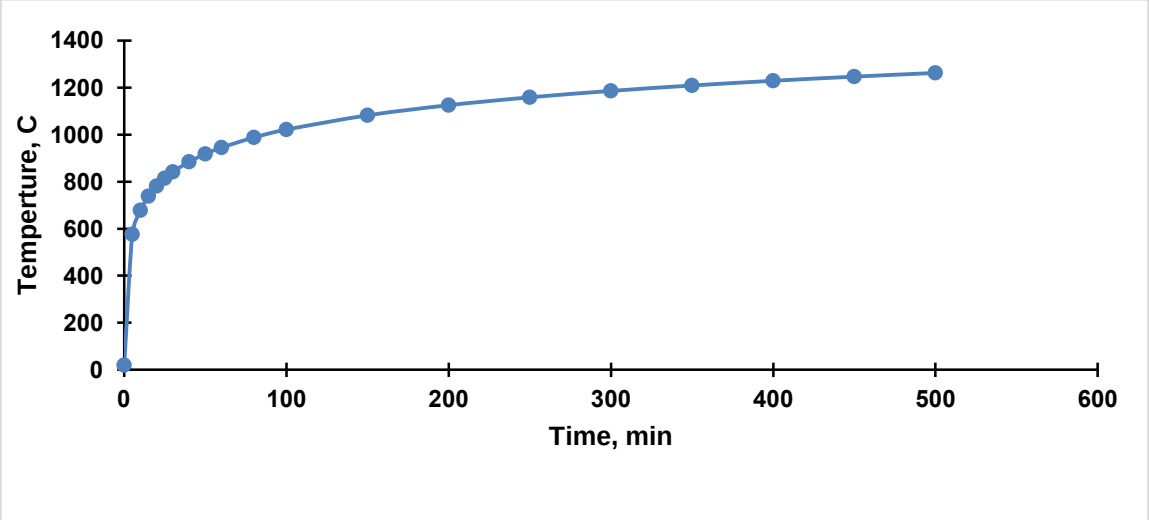

Figure 11 - Temperature versus Time curve due to fire effect (ISO-834)

Modeling of fired samples subjected to mechanical loading (the second phase)

The same methods and measurements from the prior stage are applied in this one.

Materials' characterization

There are differences in how high temperatures affect the compressive strength of concrete in the normal and high concrete classes. Equation (8) according to Yu et al. (2005a, b) [21] reflects this variation in behavior.

$$\Psi_{cT} = \frac{f_c(T)}{f_c} = \frac{1}{1 + 9 \times [(T - 20)/800]^{c_1}}, \quad (8)$$

The axial compressive strength of concrete at room temperature is symbolized by fc (T), while the axial compressive strength of concrete during high temperature can be expressed by fc. The parameter c1 in this case is 3.55 for normal concrete, while it is 6.70 for high-performance concrete (HPC).

Figure 12 in the study illustrates the relationship between elevated temperatures and the reduction in compressive strength of concrete. The figure shows that up to a temperature of 200°C, there is no significant difference in the strength reduction between normal-strength concrete and high-strength concrete. However, beyond this temperature limit, the divergence between the two curves becomes more significant until reaching 800°C. After this point, the two curves start to match each other.

Based on these observations, it can be concluded that high-strength concrete has better resistance to fire damage compared to normal-strength concrete. This means that high-strength concrete can maintain its compressive strength at higher temperatures for a longer duration before experiencing significant strength reduction compared to normal-strength concrete.

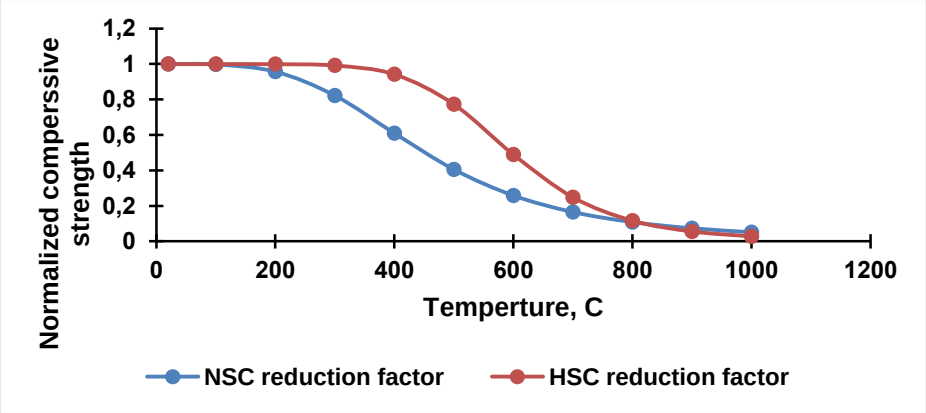

Figure 12 - Normalized residual strength of normal and high concrete class at high temperatures

Hu et al. (2014) suggested a bilinear model for calculating the tensile strength of post-fire concrete. Equation (9) was used to determine the post-fire concrete's tensile strength, expressed as ft(T) (N/mm^2) at T °C. The normalized concrete tensile strength at different high temperatures is shown in figure 13.

$$\frac{f_t(T)}{f_t} = 0.976 + [1.56 \times (\frac{T}{100}) - 4.35 \times (\frac{T}{100})^2 + 0.345 \times (\frac{T}{100})^3] \times 10^{-2} 20°C \leq T \leq 800°C \quad (9)$$

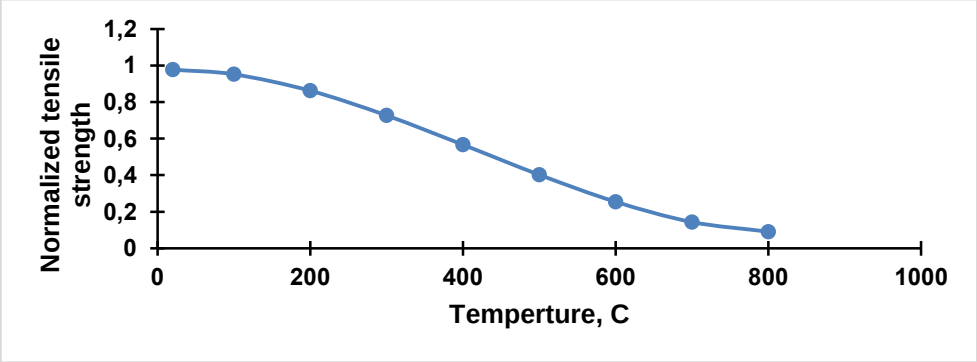

Figure 13 - Normalized residual tensile strength of concrete class under elevated temperatures

Equation (10) can be used to calculate the post-fire concrete's compression peak strain ε_0(T) at T °C. The normalized peak strain for the concrete classes with normal and high strengths is shown in figure 14. It is evident that when temperatures rise, the peak strain rises for both concrete types.

$$\varepsilon_0(T) = \{1 + c_4[(T - 20)/100]^2\}\varepsilon_0 \quad (10)$$

where the parameter c4 equals 0.037 for normal concrete and 0.017 for high-performance concrete, depending on the value of ε0, which represents the compressive strain of concrete at room temperature.

Equation (11) illustrates the relationship between strain and compression stress in post-fire concrete.

$$E_c(T) = \frac{E_c}{1+2.15\times10^{-3}[(T-20)/800]^{4.33}+3.7\times10^{-2}[(T-20)/100]^2} \quad (11)$$

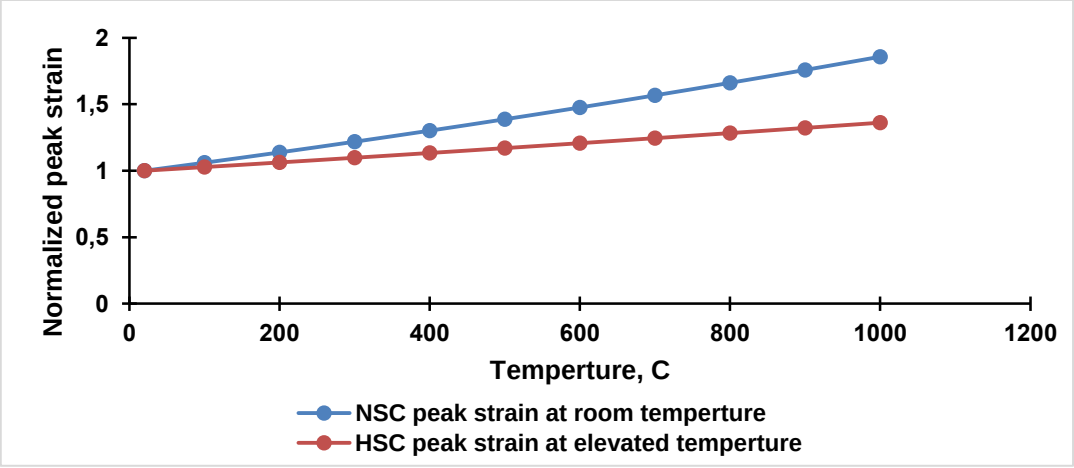

Figure 14 - Normalized strain corresponded to the maximum compressive strength of normal and high concrete class at high temperatures

Normal concrete is less resistant to high temperatures than high-class concrete. The elastic modulus of both classes can be calculated using equation (12).

At 1000°C, the elastic modulus of concrete drops to 50% of its initial value, as can be shown in figure 15.

$$y = \begin{cases} \dfrac{9.1 f_{cu}^{-4/9} x - x^2}{1 + (9.1 f_{cu}^{-4/9} - 2)x} & x \le 1 \\ \dfrac{x}{2.5 \times 10^{-5} f_{cu}^{3} (x-1)^2 + x} & x > 1 \end{cases} \qquad (12)$$

In this case, y=σc/fc(T), x=εc/ε0(T) represents the post-fire concrete's compressive stress (N/mm^2), εc its compressive strain (N/mm^2), and fcu its cube crushing strength (N/mm^2) at room temperature.

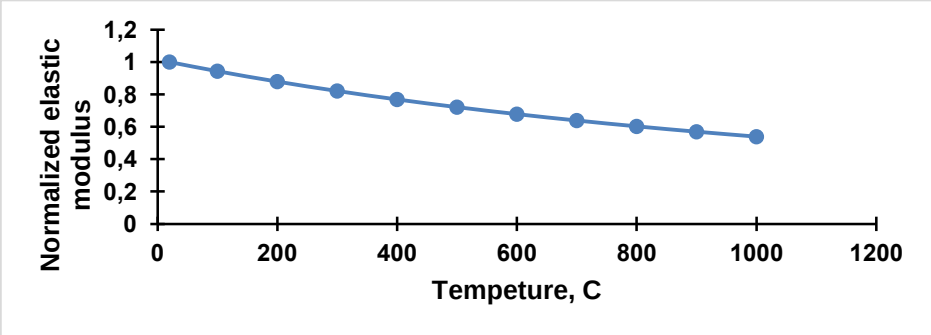

Figure 15 - Normalized concrete elastic modulus at high temperatures

The elastic modulus of post-fire concrete Ec(T) (N/ mm^2) at T°C. As shown in figure 16, it is noticeable that high exposed temperatures to concrete have a substantial negative impact on strain corresponding to peak stress and secant modulus of elasticity in addition to the concrete's compressive strength [22, 23].

Furthermore, it is evident that the material behavior's deterioration phase steepens with increasing temperature [24]. This indicates that the material's brittleness began to progressively diminish and became more ductile at higher temperatures.

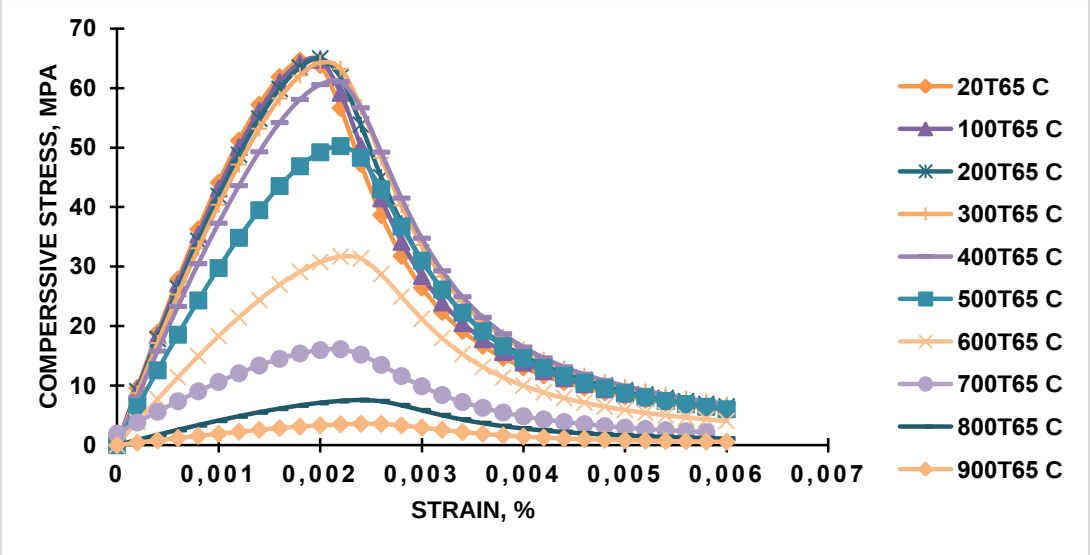

Figure 16- Compressive stress- strain behavior of normal strength concrete at various temperatures degrees

The researchers have adopted the suggested formula, described by equation (13), to assign the Poisson's ratio at elevated temperatures. Figure 17 in the study illustrates the relationship between the temperature and the corresponding Poisson's ratio values for the concrete specimens tested [25, 26].

Understanding the change in Poisson's ratio at high temperatures is essential for accurately predicting the material's behavior and deformation characteristics under fire conditions. It provides valuable insights into how the concrete responds to thermal loading and can aid in designing structures that account for these changes in mechanical properties [28].

$$\mu_\theta = a \cdot e^{-b\cdot\theta} = 0.204 \cdot e^{-0.002\cdot\theta} \quad \text{with} 20°\text{C} \leqslant \theta \leqslant 500°\text{C} \qquad (13)$$

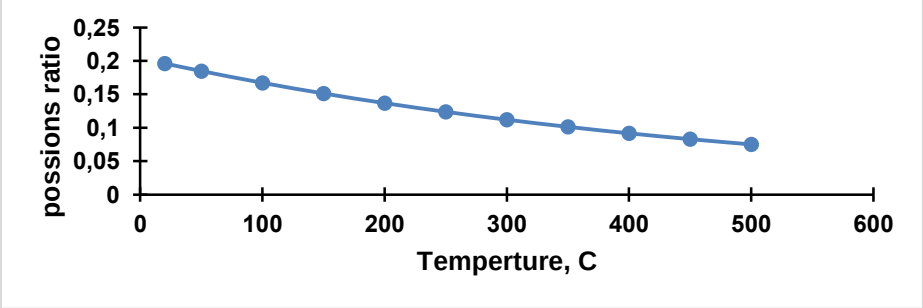

Figure 17 - Effect of high temperatures on concrete possion's ratio

Conclusions

The following findings can be drawn following an extensive and in-depth analysis of the behavior of RC concrete beams:

1. The values of residual strength of normal and high concrete differs according to the temperature. At temperature 200, they are equal to 85 Mpa. At temperature 400, their values are 50 Mpa and 80 Mpa respectively. While, at temperature 600, the values are 25 Mpa and 50 Mpa respectively. Finally, at temperature of 800 C, both types of concrete become damage without resistant to fire.
2. It is obvious that high temperatures have a negative impact on the general behavior of concrete beam, including strain and secant modulus of elasticity, in addition to the concrete's compressive strength.
3. It is clear that a material's behavior's degradation phase steepens with temperature, indicating that the material's brittleness gradually decreases and becomes more ductile at high temperatures.

REFERENCES

1. Miliozzi A., Chieruzzi M., Torre L. Experimental investigation of a cementitious heat storage medium incorporating a solar salt. *Applied Energy*. 2019. No. 250. Pp. 1023-1035.
2. Ni S., Gernay T. Predicting residual deformations in a reinforced concrete building structure after a fire event. *Engineering Structures.* 2020. Pp. 109853.
3. Khan E.U., Khushnood R.A., Baloch W.L. Spalling sensitivity and mechanical response of an ecofriendly sawdust high strength concrete at elevated temperature. *Construction and Building Materials.* 2020. No. 258. Pp. 119656.
4. Bolina F., Tutikian B., Rodrigues J.P.C. Thermal analysis of steel decking concrete slabs in case of fire. *Fire Safety Journal.* 2021. No. 121. Pp. 103295.
5. Saleheen Z., Krishnamoorthy R.R., Nadjai A. A review on behavior, material properties and finite element simulation of concrete tunnel linings under fire. *Tunnelling and Underground Space Technology*. 2022. No. 126. Pp. 104534.
6. Gao W.Y., Dai J.G., Teng J.G., Chen G.M. Finite element modeling of reinforced concrete beams exposed to fire. *Engineering structures.* 2013. No. 52. Pp. 488-501.
7. Cai B., Li B., Fu F. Finite element analysis and calculation method of residual flexural capacity of post-fire RC beams. *International Journal of Concrete Structures and Materials.* 2020. No. 14. Pp. 1-17.
8. Roudari S.S., Abu-Lebdeh T.M. Evaluation of fire effects on reinforced concrete columns using finite element method. *American Journal of Engineering and Applied Sciences.* 2019.
9. Musmar M., Shatnaw A., Shatarat N. Finite element analysis of the behavior of RC beams during fires. *ARPN Journal of Engineering and Applied Sciences.* 2018. No. 12. Pp. 6869-6876.
10. Yong W., Yu-li D., Guang-chun Z. Nonlinear numerical modeling of two-way reinforced concrete slabs subjected to fire. *Computers & Structures.* 2012. No. 119. Pp. 23-36.
11. Santosh T., Nur Y., Eyosias B. Post-fire analysis and numerical modeling of a fire-damaged concrete bridge. *Engineering Structures.* 2021. No. 244. Pp. 112764.
12. Hoang-Le M., Samir K., Magd A. A concrete damage plasticity model for predicting the effects of compressive high-strength concrete under static and dynamic loads. *Journal of Building Engineering.* 2021. No. 44. Pp. 103239.
13. Bakhti R., Benahmed B., Laib A. New approach for computing damage parameters evolution in plastic damage model for concrete. *Case Studies in Construction Materials.* 2021. No. 16. Pp. e00834.
14. Nastri E., Todisco P. Macro mechanical Failure Criteria: Elasticity, Plasticity and Numerical Applications for the Non-Linear Masonry Modelling. *Buildings.* 2022. No. 12(8). Pp. 1245.
15. Cui L., Zhang X., Hao H. Improved analysis method for structural members subjected to blast loads considering strain hardening and softening effects. *Advances in Structural Engineering*. 2021. No. 24(12). Pp. 2622-2636.
16. Kaish A.B.M.A., Alam M.R., Hassan Md.K., Ullah S.N. Numerical investigation of the behavior of retrofitted flexural cracked beam with external plate bonding. Conference: Conference on Engineering Research, Innovation and Education 2011 (CERIE 2011) At: SUST, Sylhet, Bangladesh.
17. Li W.S., Deng X.W. The temperature field finite element analysis of concrete beam after fire based on Abaqus. *Applied Mechanics and Materials*. 2011. No. 90. Pp. 3089-3092.
18. Krishna D.A., Priyadarsini R.S., Narayanan S. Effect of elevated temperatures on the mechanical properties of concrete. *Procedia Structural Integrity.* 2019. No. 14. Pp. 384-394.
19. Pokorný P., Kolísko J., Čítek D., Kostelecká M. Effect of elevated temperature on the bond strength of prestressing reinforcement in UHPC. *Materials (Basel).* 2020. No. 13(21). Pp. 4990.
20. Oliveira P.N., Fonseca E.M.M., Campilho R.D.S.G., Piloto P.A. Analytical equations applied to the study of steel profiles under fire according to different nominal temperature-time curves. *Mathematical and Computational Applications*. 2021. No. 26(2). Pp. 48.
21. Suntharalingam T., Upasiri I., Nagaratnam B., Poologanathan K., Gatheeshgar P., Tsavdaridis K.D., Nuwanthika D. Finite Element Modelling to Predict the Fire Performance of Bio-Inspired 3D-Printed Concrete Wall Panels Exposed to Realistic Fire. *Buildings.* 2022. No. 12(2). Pp. 111.
22. Bamonte P., Lo Monte F. Reinforced concrete columns exposed to standard fire: Comparison among different constitutive models for concrete at high temperature. *Fire Safety Journal.* 2015. No. 71. Pp. 310-323.
23. Weerasinghe P., Nguyen K., Mendis P., Guerrieri M. Large-scale experiment on the behaviour of concrete flat slabs subjected to standard fire. *Journal of Building Engineering.* 2020. No. 30. Pp. 101255.
24. Yang M., Pham D.T., Bleyer J., de Buhan P. Evaluating the failure load of high-rise reinforced concrete walls under fire loading using the yield design approach. *Structures.* 2023. No. 48. Pp. 934-946.
25. Dong H., Zhu J., Cao W., Rao Y., Liu Y. Structural behavior of mega steel-reinforced high-strength concrete rectangular columns under axial compression. *Journal of Building Engineering*. 2022. No. 61. Pp. 105272.

26. Roudari S.S., Abu-Lebdeh T. Evaluation of fire effects on reinforced concrete columns using finite element method. *American Journal of Engineering and Applied Sciences.* 2019. No. 12(2). Pp. 227-235.

27. Haido J.H., Tayeh B.A., Majeed S.S., Karpuzcu M. Effect of high temperature on the mechanical properties of basalt fibre self-compacting concrete as an overlay material. *Construction and Building Materials*. 2021. No. 268. Pp. 121725.

28. Alzamili H.H. Post-fire behavior of various reinforced concrete elements with various strengthening methods. Moscow. Russian Federation. 2023.

29. Elsheikh A., Alzamili H.H. Post Fire Behavior of Thesis. Peoples' Friendship University of Russia (RUDN University). Structural Reinforced Concrete Member (Slab) Repairing with Various Materials. *Civil Engineering Journal.* 2023. No. 9(8). Pp. 2012-2031. doi:10.28991/CEJ-2023-09-08-013.

СПИСОК ЛИТЕРАТУРЫ

1. Miliozzi A., Chieruzzi M., Torre L. Experimental investigation of a cementitious heat storage medium incorporating a solar salt //Applied Energy. 2019. No. 250. Pp. 1023-1035.

2. Ni S., Gernay T. Predicting residual deformations in a reinforced concrete building structure after a fire event // Engineering Structures. 2020. Pp. 109853.

3. Khan E.U., Khushnood R.A., Baloch W.L. Spalling sensitivity and mechanical response of an ecofriendly sawdust high strength concrete at elevated temperatures // Construction and Building Materials. 2020. No. 258. Pp. 119656.

4. Bolina F., Tutikian B., Rodrigues J.P.C. Thermal analysis of steel decking concrete slabs in case of fire // Fire Safety Journal. 2021. No. 121. Pp. 103295.

5. Saleheen Z., Krishnamoorthy R.R., Nadjai A. A review on behavior, material properties and finite element simulation of concrete tunnel linings under fire // Tunnelling and Underground Space Technology. 2022. No. 126. Pp. 104534.

6. Gao W.Y., Dai J.G., Teng J.G., Chen G.M. Finite element modeling of reinforced concrete beams exposed to fire // Engineering structures. 2013. No. 52. Pp. 488-501.

7. Cai B., Li B., Fu F. Finite element analysis and calculation method of residual flexural capacity of post-fire RC beams // International Journal of Concrete Structures and Materials. 2020. 14. 1-17.

8. Roudari S.S., Abu-Lebdeh T.M. Evaluation of fire effects on reinforced concrete columns using finite element method // American Journal of Engineering and Applied Sciences. 2019.

9. Musmar M., Shatnaw A., Shatarat N. Finite element analysis of the behavior of RC beams during fires // ARPN Journal of Engineering and Applied Sciences. 2018. No. 12. Pp. 6869-6876.

10. Yong W., Yu-li D., Guang-chun Z. Nonlinear numerical modeling of two-way reinforced concrete slabs subjected to fire // Computers & Structures. 2012. No. 119. Pp. 23-36.

11. Santosh T., Nur Y., Eyosias B. Post-fire analysis and numerical modeling of a fire-damaged concrete bridge // Engineering Structures. 2021. No. 244. Pp. 112764.

12. Hoang-Le M., Samir K., Magd A. A concrete damage plasticity model for predicting the effects of compressive high-strength concrete under static and dynamic loads // Journal of Building Engineering. 2021. No. 44. Pp. 103239.

13. Bakhti R., Benahmed B., Laib A. New approach for computing damage parameters evolution in plastic damage model for concrete // Case Studies in Construction Materials. 2021. No. 16. Pp. e00834.

14. Nastri E., Todisco P. Macro mechanical Failure Criteria: Elasticity, Plasticity and Numerical Applications for the Non-Linear Masonry Modelling // Buildings. 2022. No. 12(8). Pp. 1245.

15. Cui L., Zhang X., Hao H. Improved analysis method for structural members subjected to blast loads considering strain hardening and softening effects // Advances in Structural Engineering. 2021. 24(12). 2622-2636.

16. Kaish A.B.M.A., Alam M.R., Hassan Md.K., Ullah S.N. Numerical investigation of the behavior of retrofitted flexural cracked beam with external plate bonding // Conference: Conference on Engineering Research, Innovation and Education 2011 (CERIE 2011) At: SUST, Sylhet, Bangladesh.

17. Li W.S., Deng X.W. The temperature field finite element analysis of concrete beam after fire based on Abaqus // Applied Mechanics and Materials. 2011. No. 90. Pp. 3089-3092.

18. Krishna D.A., Priyadarsini R.S., Narayanan S. Effect of elevated temperatures on the mechanical properties of concrete // Procedia Structural Integrity. 2019. No. 14. Pp. 384-394.

19. Pokorný P., Kolísko J., Čítek D., Kostelecká M. Effect of elevated temperature on the bond strength of prestressing reinforcement in UHPC // Materials (Basel). 2020. No. 13(21). Pp. 4990.

20. Oliveira P.N., Fonseca E.M.M., Campilho R.D.S.G., Piloto P.A. Analytical equations applied to the study of steel profiles under fire according to different nominal temperature-time curves // Mathematical and Computational Applications. 2021. No. 26(2). Pp. 48.

21. Suntharalingam T., Upasiri I., Nagaratnam B., Poologanathan K., Gatheeshgar P., Tsavdaridis K.D., Nuwanthika D. Finite Element Modelling to Predict the Fire Performance of Bio-Inspired 3D-Printed Concrete Wall Panels Exposed to Realistic Fire / Buildings. 2022. No. 12(2). Pp. 111.

22. Bamonte P., Lo Monte F. Reinforced concrete columns exposed to standard fire: Comparison among different constitutive models for concrete at high temperature // Fire Safety Journal. 2015. No. 71. Pp. 310-323.

23. Weerasinghe P., Nguyen K., Mendis P., Guerrieri M. Large-scale experiment on the behaviour of concrete flat slabs subjected to standard fire // Journal of Building Engineering. 2020. No. 30. Pp. 101255.

24. Yang M., Pham D.T., Bleyer J., de Buhan P. Evaluating the failure load of high-rise reinforced concrete walls under fire loading using the yield design approach // Structures. 2023. No. 48. Pp. 934-946.

25. Dong H., Zhu J., Cao W., Rao Y., Liu Y. Structural behavior of mega steel-reinforced high-strength concrete rectangular columns under axial compression // Journal of Building Engineering. 2022. No. 61. Pp. 105272.

26. Roudari S.S., Abu-Lebdeh T. Evaluation of fire effects on reinforced concrete columns using finite element method // American Journal of Engineering and Applied Sciences. 2019. No. 12(2). Pp. 227-235.

27. Haido J.H., Tayeh B.A., Majeed S.S., Karpuzcu M. Effect of high temperature on the mechanical properties of basalt fibre self-compacting concrete as an overlay material // Construction and Building Materials. 2021. No. 268. Pp. 121725.

28. Alzamili H.H. Post-fire behavior of various reinforced concrete elements with various strengthening methods // Thesis. Peoples' Friendship University of Russia (RUDN University). Moscow. Russian Federation. 2023.

29. Elsheikh A., Alzamili H.H. Post Fire Behavior of Structural Reinforced Concrete Member (Slab) Repairing with Various Materials // Civil Engineering Journal. 2023. No. 9(8). Pp. 2012-2031. doi:10.28991/CEJ-2023-09-08-013.

Information about authors:

Alzamili Hadeal Hakim
Peoples' Friendship University of Russia (RUDN University), Moscow, Russia,
PhD student department of Civil Engineering, Academy of Engineering.
E-mail: HadealHakim8@gmail.com

Elsheikh Asser Mohamed
Peoples' Friendship University of Russia (RUDN University), Moscow, Russia,
candidate in technical sciences, assistant professor department of Civil Engineering, Academy of Engineering.
Mansoura University, Mansoura, Egypt,
candidate in technical sciences, associated professor.
E-mail: elsheykh_am@pfur.ru

Информация об авторах:

Альзамили Хадиль Хаким
Российский университет дружбы народов (РУДН), г. Москва, Россия,
аспирантка департамента строительства инженерной академии.
E-mail: HadealHakim8@gmail.com

Эльшейх Ассер Мохамед
Российский университет дружбы народов (РУДН), Москва, Россия,
кандидат технических наук, доцент департамент строительства инженерной академии.
Мансура университет, Мансура, Египет,
кандидат технических наук, доцент.
E-mail: elsheykh_am@pfur.ru